



Pitts et al., 2003; Kleffmann et al., 1998]. Since water vapor and surface adsorbed water are closely related to each other, it is difficult to assess the role of water in the different laboratory experiments. Attempts to explain the formation of HONO typically assume that the dependence is on surface adsorbed water [Finlayson-Pitts et al., 2003; Jenkin et al., 1988].

[8] Based on these observations the following stoichiometry for NO<sub>2</sub> to HONO conversion has been suggested:



[9] Besides the phenomenological descriptions of the NO<sub>2</sub> to HONO conversion via reaction (R1), we know very little about the detailed molecular processes. Jenkin et al. [1988] proposed a reaction mechanism in which a H<sub>2</sub>O NO<sub>2</sub> water complex on the surface reacts with a gas-phase NO<sub>2</sub> molecule. In a more recent publication, Finlayson-Pitts et al. [2003] proposed a mechanism that proceeds through N<sub>2</sub>O<sub>4</sub> adsorbed on surface films where it isomerizes to the asymmetric form, ONONO<sub>2</sub>. Whether the formation of the N<sub>2</sub>O<sub>4</sub> occurs in the gas-phase, followed by an uptake onto the surface, or directly on the surface is currently unclear. The ONONO<sub>2</sub> autoionizes to NO<sup>+</sup>NO<sub>3</sub><sup>-</sup>, which reacts with surface adsorbed water to generate HONO and HNO<sub>3</sub>. HONO can then escape into the gas phase or undergo secondary reactions. While evidence for certain steps of this mechanism has been observed in the laboratory [Barney and Finlayson-Pitts, 2000], most observations were made at NO<sub>2</sub> levels far above typical ambient concentrations. It remains to be seen whether this mechanism can explain the HONO levels observed in the atmosphere.

[10] A number of other HONO formation mechanisms have been suggested. Some researchers have suggested a reaction stoichiometry according to reaction (R2) [Andres-Hernandez et al., 1996; Calvert et al., 1994; Sjödin and Ferm, 1985], but many laboratory and field studies have observed high formation rates of HONO in the absence of NO [Alicke et al., 2002; Kleffmann et al., 1998; Platt, 1986; Svensson et al., 1987], thus making it unlikely that this mechanism plays a role in the atmosphere:



[11] Saliba et al. [2000, 2001] recently proposed that the reaction of NO with surface adsorbed HNO<sub>3</sub> releases gas-phase HONO, but the mechanism appears to play a role only under conditions with very high NO concentrations. Recent studies [Ammann et al., 1998; Gerecke et al., 1998; Kalberer et al., 1999; Kleffmann et al., 1999; Longfellow et al., 2000] also point at soot particles as a possible surface for the formation of HONO. While the formation rate seems to be fast in the first minute of exposure with NO<sub>2</sub>, a passivation of the surface rapidly slows down the formation afterwards.

[12] HONO is also produced directly in various combustion processes. Earlier studies [Kessler, 1984; Pitts et al., 1984a] found that the [HONO]/[NO<sub>x</sub>] emission ratio from automobiles varied between 0.1 and 1%. Recent traffic tunnel studies in the United States and Germany found average [HONO]/[NO<sub>x</sub>] values ranging from 0.3% to 0.8% [Ackermann, 2000; Kirchstetter et al., 1996; Kurtenbach et al., 2001].

[13] A number of parameterizations of the NO<sub>2</sub> to HONO conversion rate have been presented. Svensson et al. [1987] propose a rate of formation based on their observations in a glass reactor that depends on NO<sub>2</sub> and gas-phase water concentrations, as well as the surface to volume ratio. Lammel [1999] introduced a similar parameterization of the formation of HONO, which is based on surface type and a relative humidity specific surface to volume ratio, thus expanding the concept introduced by Svensson et al. [1987] (see below for more details). Kleffmann et al. [1998] derived a reactive uptake coefficient for NO<sub>2</sub> of  $10^{-6}$  on a surface with adsorbed water. In a recent study, Kurtenbach et al. [2001] determined the NO<sub>2</sub>-HONO conversion frequency on a concrete traffic tunnel wall with a surface to volume ratio of 1 m<sup>-1</sup> to be  $5 \cdot 10^{-5} \text{ s}^{-1}$ .

[14] Only a few investigations have studied the water dependence of HONO formation in the atmosphere. While not analyzed in detail, the observations of Harris et al. [1982] appear to show a weak dependence of the nocturnal [HONO]/[NO<sub>2</sub>] ratio on relative humidity (RH). Sjödin and Ferm [1985] found a correlation of their 12h integrated denuder measurements of HONO mixing ratios with the product of [NO][NO<sub>2</sub>][H<sub>2</sub>O], based on the mechanism in reaction (R2). It is difficult to assess the role of water, in particular since it is believed today that the mechanism in reaction (R2) does not play a major role in the formation of HONO under normal atmospheric conditions. A similar argument applies to the data shown by Calvert et al. [1994]. The most detailed information on the role of water can be found in the work of Lammel [1999], who parameterizes the formation of HONO by classifying surfaces as ~~dry, wet, and aqueous~~ <sup>dry, wet, and aqueous</sup>. For most surfaces, ~~dry~~ <sup>dry</sup> was defined as the surface state below a limiting RH, for example, 50% RH for urban surfaces. ~~Wet~~ <sup>Wet</sup> surfaces of insoluble material, i.e., soil, occurred at a RH range that was limited by the transition to ~~dry~~ <sup>dry</sup> surfaces at the lower end and 95% at the upper end. Insoluble surfaces above 95% RH and soluble aerosol above their deliquescence point or crystallization point, depending on their history, were classified as ~~aqueous~~ <sup>aqueous</sup> surfaces. Lammel [1999] then parameterized the HONO formation rate, P<sub>HONO</sub>, on all surfaces, with the exception of soot particles, with the following equation (here only given for nonsoot surfaces):

$$P_{\text{HONO}} \propto \frac{1}{V} \left( \frac{S_{\text{dry}}}{V} \right)^{\frac{1}{2}} \left( \frac{S_{\text{aqueous}}}{V} \right)^{\frac{1}{2}} k^{\text{het01b}} \propto \frac{S_{\text{wet}}}{V} k^{\text{het02b}} \quad \text{H}_2\text{O} : \quad \text{R3b}$$

[15] The equation is based on a pseudo-first order behavior for ~~dry and aqueous~~ <sup>dry and aqueous</sup> surfaces, which makes the HONO formation independent of [H<sub>2</sub>O] with a first order rate coefficient  $k^{\text{het(1)}}$ . In the case of a ~~wet~~ <sup>wet</sup> surface, equation (3) becomes dependent on the water concentration with a second-order rate coefficient of  $k^{\text{het(2)}}$ . This parameterization is based on the argument that the amount of chemisorbed water at very dry conditions becomes approximately independent of the water vapor levels, while in a ~~wet~~ <sup>wet</sup> phase (above 1 monolayer of H<sub>2</sub>O) the amount of adsorbed water is dependent on water vapor.

[16] The nonphotolytic loss of HONO also plays an important role in the nocturnal atmosphere. A number of

atmospheric observations [Harrison et al., 1996; Kitto and Harrison, 1992; Spindler et al., 1999; Stutz et al., 2002] and laboratory investigations [Bongartz et al., 1994; Kaiser and Wu, 1977; Mertes and Wahner, 1995; Pitts et al., 1984b; Sakamaki et al., 1983; Svensson et al., 1987; TenBrink and Spoelstra, 1998] have studied the fate of HONO in the dark. All studies report that the loss of HONO in the atmosphere proceeds via heterogeneous reactions or surface uptake. One proposed reaction mechanism has the stoichiometry:



[17] Several studies have reported that reaction (R4) occurs as a second-order reaction on the surfaces of the respective reaction vessels [Kaiser and Wu, 1977; Sakamaki et al., 1983; Svensson et al., 1987; TenBrink and Spoelstra, 1998] with rate constants of  $10^{-22} \text{ cm}^3 \text{ molec}^{-1} \text{ s}^{-1}$  for a passivated surface [Svensson et al., 1987] and  $1.5 \cdot 10^{-19} \text{ cm}^3 \text{ molec}^{-1} \text{ s}^{-1}$  in a Teflon smog chamber [TenBrink and Spoelstra, 1998]. At these rates, destruction of HONO in the atmosphere would be too slow to be significant. Recently, Syomin et al. [2002] suggested, based on laboratory observations, a different mechanism in the presence of surface adsorbed  $\text{HNO}_3$ :



The order of the HONO loss is, however, unclear.

[18] It is clear from the existing literature that a dependence of HONO chemistry on gas phase or adsorbed water can be expected. Most studies, however, have been made in laboratory environments on surfaces that may not be representative for atmospheric conditions. The water dependence in the real atmosphere has thus far not been extensively studied. Here we present nocturnal HONO and  $\text{NO}_2$  data from three field experiments in environments with different RH. Humid data was obtained in Nashville during the Southern Oxidant Study in 1999 and during the Texas Air Quality Study in Houston, Texas in 2000. Much drier conditions were observed in Phoenix, Arizona during an experiment in 2001. The three data sets are analyzed with respect to the conversion of  $\text{NO}_2$  to HONO in the nocturnal atmosphere using a pseudo steady state approach. Conclusions about the dependence of the net  $\text{NO}_2$  to HONO conversion mechanism on the RH in the urban environment are drawn.

## 2. Experimental Procedure

[19] All  $\text{NO}_2$  and HONO data presented here were measured by long-path differential optical absorption spectroscopy (DOAS) [Platt, 1994]. The University of California, Los Angeles DOAS system consists of a telescope that sends and receives a collimated light beam. The beam is folded once by an array of quartz corner cube retroreflectors. Spectroscopic detection is achieved by a spectrograph detector system coupled to the telescope. A detailed description of the basic setup and the analysis method can be found in the work of Alicke et al. [2003]. To achieve low detection limits, the telescope and the retroreflector array were separated by 1.5 km. In addition, the retroreflector array was mounted at a different altitude than the telescope. The DOAS

light beam therefore integrated over a volume of air that extended both in the horizontal and the vertical. Measurements of RH were made by standard meteorological instruments in all cases. The NO data used in the analysis was determined by chemiluminescence instruments.

[20] We present here data from three field experiments at different locations in the United States. All three experiments were performed during summer, with relatively high temperatures.

### 2.1. SOS 1999

[21] In June and July 1999, during the Southern Oxidant Study experiment in Nashville, Tennessee, we deployed our DOAS system in a suburban area 8 km northeast of downtown Nashville. The main ground site, the Cornelia Fort airfield, was located in the 30 m deep and 1.5 km wide Cumberland River valley. The DOAS telescope was set up in the valley and aimed at a retroreflector array located at a building on the opposite valley ridge. The data were measured on a light path of 1.35 km single length, extending from 2 to 35 m altitude above the valley ground. The light path integrated over the entire cross section of the valley. The valley floor was a mixture of grass, trees, and concrete. No direct sources of  $\text{NO}_x$  and HONO were located in the valley. The airport was operated infrequently and was closed at night. Roads were located on both ridges of the valley. The nocturnal conditions in the valley were generally humid, often reaching RH of 100%. We also frequently observed ground fog. Measurements of RH were made with a Vaisala HMP45C humidity probe in 2 m altitude. NO was measured by a chemiluminescence instrument [Williams et al., 1998] 10 m above the ground. Winds in the valley were typically slow at night, and vertical mixing was weak.

### 2.2. TEXAQS 2000

[22] During the Texas Air Quality Study in August and September 2000 our instrument was set up at the ground at the La Porte airport, 20 km southeast of downtown Houston. Although we measured on several different light paths, we will only use the data of the light path aiming at a retroreflector array placed on top of a water tower at 1.9 km distance. The path averaged over an altitude interval from 2 to 44 m. The area under the light path was a mixture of concrete, grass, trees, and house roofs. The immediate location around the airport had little traffic, and the airfield was only rarely used during the night. However, larger chemical refineries were located at a distance of 3–4 km, thus influencing the site at certain wind directions. RH and NO were measured in approximately 750 m distance from the light path by a Vaisala HMP45C humidity probe 2 m above ground and a chemiluminescence instrument [Williams et al., 1998] at 10 m altitude, respectively. During this campaign, nocturnal RH was in the range from 50 to 100%. Winds were generally stronger than in Nashville, and the air at night was vertically better mixed.

### 2.3. Phoenix 2001

[23] The setup during the Phoenix Sunrise experiment in June 2001 was different from the first two campaigns. While the DOAS telescope was located on the ground in Nashville and Houston, it was placed on the top of the highest building in downtown Phoenix, at an altitude of 139 m above the ground. Retroreflectors were mounted at a

distance of 3.3 km on the roof of three buildings, at altitudes of 10, 45, and 110 m agl. The DOAS telescope was aimed consecutively onto the individual retroreflector arrays, measuring on all three light paths within 15 min.

[24] Because of the influence of vertical mixing on HONO levels [Stutz et al., 2002], it is difficult to compare the path integrated data averaging from 10 m to 139 m height directly with the results from the other studies that integrated over much smaller height intervals. We have therefore used the data from the 45–139 m and 10–139 m light paths to calculate the trace gas concentrations in the 10–45 m height interval [Wang et al., 2003b]. In short, we linearly interpolated the data of the 45–139 m light path to the time of the 10–139 m light path measurements. In this process, we filtered out periods where fast temporal concentration changes would have made a subtraction of the data on the two light paths unreliable. The 10–45 m interval concentration is then derived by scaling the 45–139 m concentrations with the length of the 10–139 m path between 45 and 139 m, followed by a subtraction of this value from the 10–139 m path trace gas levels. The result are the trace gas concentrations in the height interval of 10–45 m with a horizontal length of 0.9 km. Owing to the possible influence of temporal concentration changes between the two light paths that escaped the filtering procedure, the 10–45 m data can show larger temporal variations.

[25] The area under the light paths in Phoenix was covered by buildings, roads, and some vegetation. Most of the buildings were about 2½ stories high with a few exceptions of higher structures. This mixture of ground and roofs leads to an average altitude of the reactive ground surface that is higher than the ground. Thus the retroreflector mounted on the roof of a three-story building at 10 m agl was closer to the reactive surface than the height above the ground suggests.

[26] The vegetation in Phoenix was sparser than at the other two locations. Another difference between Phoenix and the other experiments was the larger direct emissions due to traffic. In particular, after 0500 local time the morning rush hour introduced large amounts of NO<sub>x</sub> and HONO into the boundary layer. The strongest nocturnal source was the I10 freeway, which crossed the light beam close to the location of the telescope. Because the 10–45 m interval was located at a distance of ~2 km from the freeway, direct emissions should not have a large impact on the data.

[27] Measurements of NO, which are later used to calculate the significance of direct emission as a HONO source, were performed at the 16th floor of the building hosting the DOAS telescope at 50 m agl. This altitude is above the 10–45 m interval of the DOAS data. We therefore have to consider that during the night the concentration measurements of NO, which is emitted at the ground, will most likely underestimate the NO levels between 10 and 45 m due to the weak vertical mixing and the reaction with ozone. The NO monitor was located at a distance of ~2.4 km from the DOAS measurement volume. Although the different locations of the probed volumes could introduce uncertainties in our analysis, a comparison of the DOAS and in situ O<sub>3</sub> data measured at the same location as NO shows that the agreement is, in general, good.

[28] Meteorological measurements were made at an altitude of 45 m agl at the rooftop of a building with a

Table 1. Time Frame and Measurement Characteristics of the Three Field Experiments

	Time Frame	Height Interval, m	Relative Humidity Range, %
SOS99 Nashville	6/18/99–7/12/99	2–45	50–90
TexAQs 2000	8/24/00–9/11/00	2–4	35–90
Phoenix 2001	6/17/01–6/30/01	10–45	10–70

Campbell weather station. Comparison with other measurements close to the ground (not shown here) gives us confidence that the RH measurements at 45 m altitude are representative for the 10–45 m height interval. Our measurements show that the nights in Phoenix were very dry. With the exception of the night of 25–26 June, the RH never exceeded 50%. On 25 June the RH climbed up to 70%, comparable to the observations in Nashville and Houston. Details of the light path geometries during the three field experiments, as well as the various meteorological conditions, are summarized in Table 1.

[29] Since our study is focused on the chemical formation of HONO, it is necessary to separate direct HONO emissions from HONO that is formed through the conversion of NO<sub>2</sub>. We estimated the concentration of HONO that is emitted from traffic from the observed NO<sub>x</sub> levels and the emission ratio of 0.003 measured by Kirchstetter et al. [1996] for a typical U.S. car fleet in a traffic tunnel and subtracted this value from the observed HONO concentrations, [HONO]<sub>obs</sub>.

$$[HONO] = [HONO]_{obs} - 0.003 [NO_x] \quad (6)$$

[30] Equation (6) is based on the assumption that directly emitted HONO is not lost after emission. This is clearly incorrect for HONO emissions during the day, when photolysis will destroy HONO. Additionally, nocturnal NO<sub>x</sub> levels emitted before sunset should, in principle, not be considered in equation (6). Since it is difficult to determine the time of the NO<sub>x</sub> emissions, in particular later during the night, we will use 0.003 [NO<sub>x</sub>] as an upper estimate of the contribution of direct HONO emissions. As mentioned above, HONO can also be lost heterogeneously during the night. This process will also reduce the contribution of direct HONO emissions in equation (6). We will thus interpret [HONO] as the lower limit of the amount of chemically formed HONO, while the uncorrected observation, [HONO]<sub>obs</sub>, is the upper limit. To illustrate the possible effect of direct HONO emissions we will use both, [HONO]<sub>obs</sub> and [HONO] throughout most of this paper.

### 3. Results

[31] We chose four example nights from the three locations (Nashville, Houston, and Phoenix) to illustrate the behavior of [NO<sub>2</sub>] and [HONO] during the night (Figures 1–4). The figures also contain information about the relative humidity and [NO]. The latter is needed for the correction of direct HONO emissions by equation (6). We begin with discussing two humid nights from Nashville and Houston.

[32] The RH in Nashville (Figure 1) increased from a sunset value of ~60% to 95–100% in the second half of the night. The night of 12–13 July 1999 had very low NO



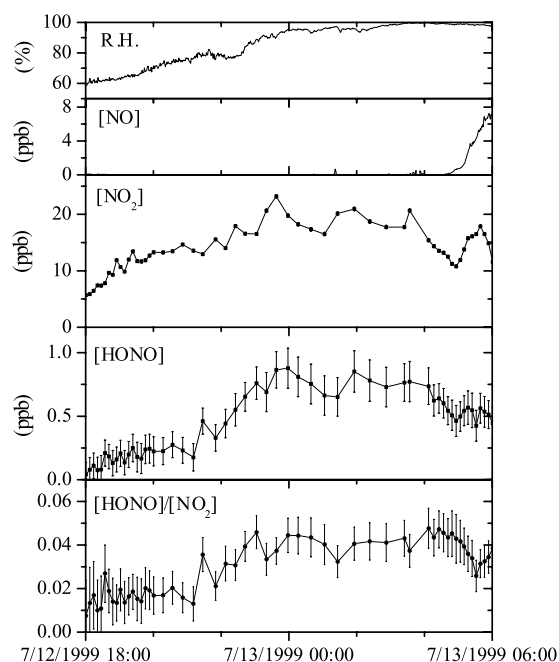


Figure 1. Behavior of [NO], [NO<sub>2</sub>], [HONO], and relative humidity (RH) during one night in Nashville, Tennessee. Sunrise is around 0530. [HONO]<sub>obs</sub> was not statistically different from [HONO] and was thus omitted in the graph.

levels. The increase of [NO] in the morning was caused by the beginning photolysis of NO<sub>2</sub> at sunrise and the onset of the rush hour. The NO<sub>2</sub> levels in Nashville increased slightly from sunset to midnight but stayed constant at

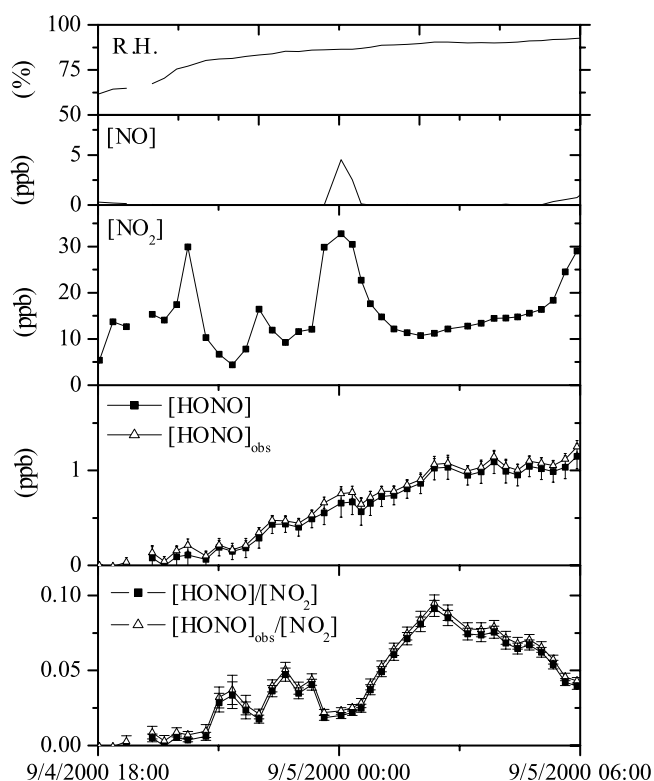


Figure 2. Behavior of [NO], [NO<sub>2</sub>], [HONO], and RH during one night in Houston, Texas.

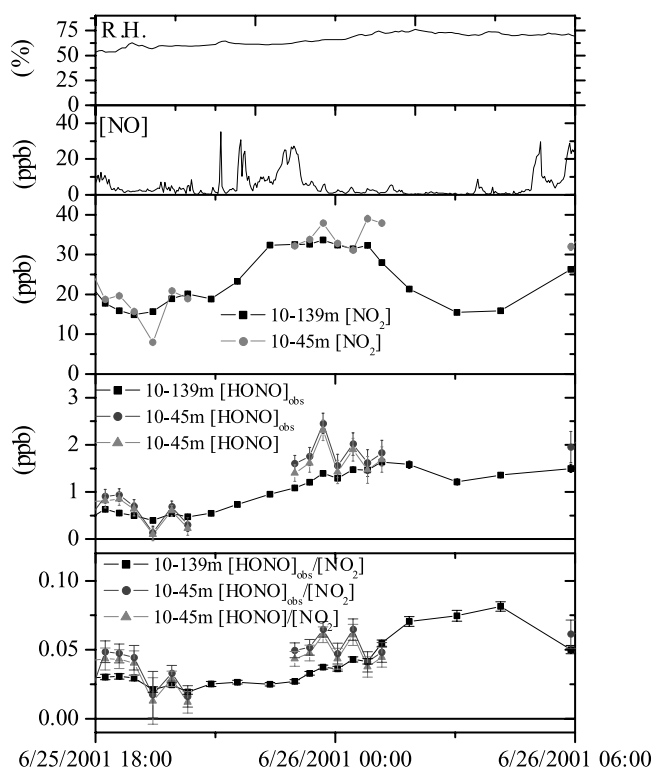


Figure 3. Behavior of [NO], [NO<sub>2</sub>], [HONO], and RH during one night in Phoenix, Arizona. The night is characterized by relatively high nocturnal RH. See color version of this figure at back of this issue.

20 ppb afterward (Figure 1). HONO mixing ratios started to increase right after sunset and reach a maximum level of 0.8 ppb at midnight, after which [HONO] stayed fairly constant until sunrise around 0530. During this night in Nashville, the correction of direct HONO emissions was negligible. The [HONO]/[NO<sub>2</sub>] ratio in Nashville showed a similar temporal behavior as [HONO] due to the relatively constant NO<sub>2</sub> levels. The maximum [HONO]/[NO<sub>2</sub>] ratio reached during this night was 5%.

[33] The behavior of the RH in Houston (Figure 2) during the night of 4–5 September 2000 is similar to that in Nashville (Figure 1). NO levels in Houston were low, except for one plume event around midnight. This plume is also reflected in the increase of NO<sub>2</sub> mixing ratios at midnight. The normal NO<sub>2</sub> levels in Houston were between 10 and 20 ppb, somewhat lower than in Nashville, except for the two plumes at 2000 and 0000 hours (Figure 2). As in Nashville (Figure 1), HONO mixing ratios in Houston started to increase right after sunset and reached a maximum of 1 ppb at 0230. We included both the observed HONO, [HONO]<sub>obs</sub>, and emission-corrected HONO, [HONO], data in Figure 2 to illustrate the effect of the correction with equation (6). The difference between [HONO] and [HONO]<sub>obs</sub> was 10%. The [HONO] build-up showed a leveling off at 0230 and [HONO] remained constant from 0230 to 0600. The behavior of the [HONO]/[NO<sub>2</sub>] ratio in Houston is not as clear, since the two plumes with elevated [NO<sub>2</sub>] and [NO] lead to a dip in the [HONO]/[NO<sub>2</sub>] ratio. We suspect that the plumes originated from a nearby industrial source. It is likely that a conversion of NO<sub>2</sub> to HONO in the

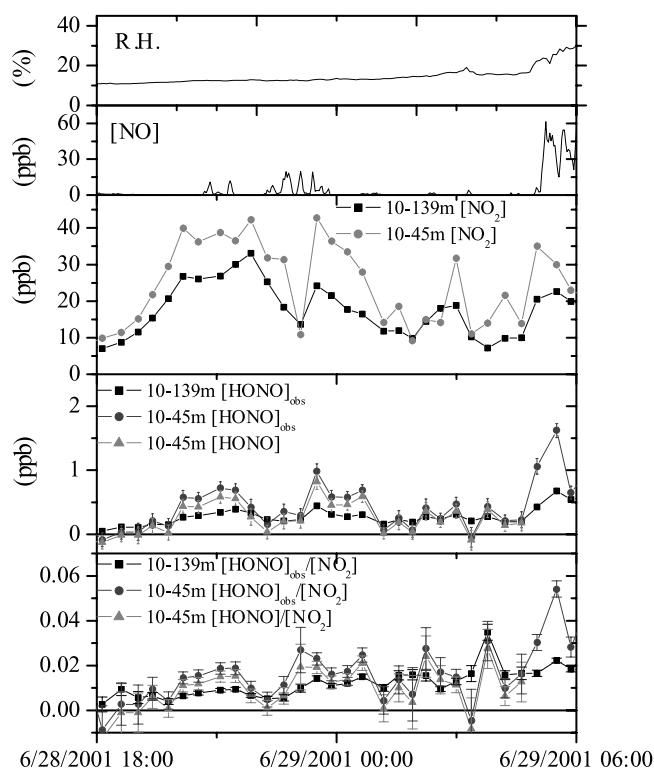


Figure 4. Behavior of [NO], [NO<sub>2</sub>], [HONO], and RH during one night in Phoenix, Arizona. The night is characterized by very low nocturnal RH below 35%. [HONO] is not shown after 0430, when the onset of photolysis and strong emissions during rush hour make an emission correction unreliable. See color version of this figure at back of this issue.

relatively freshly polluted air masses has not yet proceeded as far as in other air masses, thus leading to [HONO]/[NO<sub>2</sub>] ratios more like those encountered at the beginning of the night. Despite the larger variation of [HONO]/[NO<sub>2</sub>], a clear trend of increasing ratios towards a maximum of 8% was observed. The ratio decreases somewhat after this maximum to a value of 6%.

[34] Both nights in Nashville and Houston have in common that HONO mixing ratios level off and remain constant in the second part of the night. We have observed this leveling off of [HONO] in other locations [Stutz et al., 2002] and believe it is a common feature of the NO<sub>2</sub> to HONO conversion in urban areas.

[35] Two nights from our measurements in Phoenix are shown in Figures 3 and 4. The figures are organized in a similar way as those of Nashville and Houston. The large gaps in the 10–139 m [NO<sub>2</sub>] and [HONO] data in Figure 3 are caused by the poor time resolution and problems in the calculation of the 10–139 m data. To bridge these gaps, we have also included the original long path data averaged over a height interval of 10–139 m. Because [NO<sub>2</sub>] and [HONO] generally showed larger mixing ratios near the ground in Phoenix, the 10–139 m data can be considered as a lower estimate for the 10–45 m values.

[36] Phoenix typically has a much dryer climate during the early summer than Nashville or Houston. Nocturnal RH

often does not exceed 20%. We have, however, encountered one night during our measurements in Phoenix (25 June 2001) when the RH increased to 70% (Figure 3). NO mixing ratios during this night were generally below 5 ppb, except for a period between 2100 and midnight and after sunrise. The high NO levels before midnight were not reflected in any of the DOAS data, and we suspect that the in situ monitor observed an air mass that was transported locally, for example from the street canyon under the sampling site. [NO<sub>2</sub>] varied slowly between 20 and 30 ppb. Little difference was seen between the path-averaged and 10–139 m NO<sub>2</sub> mixing ratios, indicating that the air was vertically fairly well mixed. This night started out with relatively high [HONO] and [HONO]/[NO<sub>2</sub>] due to a dense cloud cover during the afternoon that reduced HONO photolysis and thus increased HONO mixing ratios. Despite the higher starting levels of [HONO], we observed an increase of [HONO] and [HONO]/[NO<sub>2</sub>] until 0200 to about 1.5 ppb and 0.06, respectively, in the 10–45 m height interval. In general, the data in the 10–45 m height interval were slightly higher than the path-averaged values. Because the 10–45 m data between 2000 and 2300 and after 0200 are missing, we will use the path-averaged data as lower limits for [HONO]<sub>obs</sub> and [HONO]<sub>obs</sub>/[NO<sub>2</sub>]. The path-averaged HONO data showed a leveling off after 0200. This was also reflected in the [HONO]/[NO<sub>2</sub>] data, which leveled off at a value of 0.08. The emission-corrected HONO, [HONO], which is only shown for the 10–45 m data, was up to 10% lower than the direct HONO observations, [HONO]<sub>obs</sub>. The behavior of [HONO], in particular the leveling off of the [HONO]/[NO<sub>2</sub>] values at 0.06–0.08 at 0200, was similar to our example nights in Nashville and Houston. We attribute this to the relatively high RH of 70% during the second half of the night in Phoenix.

[37] Most nights in Phoenix, however, were rather dry. The night of 28 June 2001 (Figure 4) showed a RH after sunset of 10%, which increased only slowly throughout the night. NO mixing ratios were below 10 ppb and only increased after sunrise and the onset of traffic in the morning. NO<sub>2</sub> mixing ratios in the 10–45 m height interval were 40 ppb before midnight and decreased to values between 10 and 20 ppb later during the night. A comparison with the path-integrated data shows that the levels of [NO<sub>2</sub>] close to the ground were higher during this night, implying that vertical mixing was weak. As for [NO<sub>2</sub>], [HONO] levels showed considerable differences between the 10–139 m path averaged and the 10–45 m data, in particular in the first half of the night. At the beginning of the night there was also a 10% difference between observed and emission-corrected HONO values. Later in the night, both values agreed better due to the lower NO<sub>x</sub> levels. Although the [HONO] data showed considerable temporal changes, it appeared that an increase of [HONO] and [HONO]/[NO<sub>2</sub>] was observed during the first half of the night. After midnight [HONO]/[NO<sub>2</sub>] did not increase further, and remained at an average below 0.015, with maximum values of 0.03. [HONO] levels were below 0.5 ppb during this time. After 0500 the contributions of traffic emissions of NO, NO<sub>2</sub>, and HONO, as well as the onset of photolysis at sunrise, were observed.

[38] It is interesting to compare the two nights in Phoenix shown in Figures 3 and 4. Both nights showed [NO<sub>2</sub>] levels

between 10 and 40 ppb in the 10<sup>15</sup> m interval. Both nights also showed high [NO<sub>2</sub>] values before midnight and lower values after midnight. The behavior of [HONO] and [HONO]/[NO<sub>2</sub>], however, was drastically different between the two nights. While during the night of 25<sup>26</sup> June 2001 [HONO] steadily increased to 1.5<sup>22</sup> ppb, HONO values remained below 0.8 ppb on 28<sup>29</sup> June 2001. This becomes even more clear if one compares the [HONO]/[NO<sub>2</sub>] data, which reached up to 0.08 during the first night but only 0.03 on 28<sup>29</sup> June 2001. The main difference between these two nights was the much higher RH during the night of 25<sup>26</sup> June 2001. Vertical mixing may have played a role in the first part of the night of 28<sup>29</sup> June 2001, but a comparison of the path-averaged and 10<sup>15</sup> m data showed that the air was better mixed in the second part of the night.

#### 4. Discussion

[39] The phenomenological description of the different behavior of HONO in humid and dry nights in Figures 1 to 4 is a first step in the understanding of the influence of RH on HONO chemistry. In the following section, we continue to derive a more statistical description of RH influence on HONO chemistry.

##### 4.1. Theoretical Consideration

[40] To understand the behavior of the NO<sub>2</sub>-HONO system in more detail and to provide a theoretical basis for the interpretation of our observations, we will first develop a simple analytical description of the temporal behavior of [HONO]. The chemical formation of HONO will be described as a first order process in NO<sub>2</sub> occurring on surfaces with a surface area, S, to air volume, V, ratio of (S/V) [Finlayson-Pitts et al., 2003; Jenkin et al., 1988; Kleffmann et al., 1998; Pitts et al., 1984b; Sakamaki et al., 1983; Svensson et al., 1987]. We incorporate the influence of water observed in various laboratory studies [Finlayson-Pitts et al., 2003; Jenkin et al., 1988; Kleffmann et al., 1998] by using a RH-dependent reactive conversion probability  $g_{\text{NO}_2 \rightarrow \text{HONO}}(\text{RH})$ , without further specifying the functional dependence on RH. The second process influencing HONO concentrations is the heterogeneous loss of HONO. We assume a loss that is first order in HONO. Evidence for this reaction order will be given below. Whether the HONO loss depends on the surface adsorbed water is unknown. In analogy to the observed water dependence of NO<sub>2</sub> and HNO<sub>3</sub> uptake [Finlayson-Pitts et al., 2003; Saliba et al., 2001], we will assume that HONO also has a RH-dependent uptake probability,  $g_{\text{HONO}}(\text{RH})$ . A RH dependence was recently observed by Syomin and Finlayson-Pitts [2003], between 0% and 50% RH. Equation (7) describes this simple model mathematically [Finlayson-Pitts and Pitts, 2000]:

$$\frac{d[\text{HONO}]}{dt} = \frac{S}{V} \frac{v_{\text{NO}_2}}{4} [\text{NO}_2] g_{\text{NO}_2 \rightarrow \text{HONO}}(\text{RH}) - \frac{S}{V} \frac{v_{\text{HONO}}}{4} [\text{HONO}] g_{\text{HONO}}(\text{RH}) \quad (7)$$

[41] Here  $v_{\text{NO}_2}$  and  $v_{\text{HONO}}$  are the mean molecular velocities of the respective species. At the beginning of

the night, when HONO levels are generally low, the first term in equation (7) dominates, and equation (7) predicts an increase in [HONO]. As the night proceeds and HONO accumulates, the HONO loss term will gain importance, counterbalancing the formation rate, thus ultimately leading to a pseudo steady state and constant [HONO] as observed in Figures 1<sup>22</sup>

[42] By further simplifying equation (7), we can derive an analytical expression for the temporal behavior of the [HONO]/[NO<sub>2</sub>] ratio. We will assume that the change of [NO<sub>2</sub>] due to the conversion to HONO and other reactions is small. We therefore assume that the NO<sub>2</sub> concentration is constant with time. Since the mean velocities of NO<sub>2</sub> and HONO only differ by 2%, we will set both to  $v$  for the following calculation. Another simplification in our equation is that we consider the reaction probabilities and S/V to be time independent, although we know that both parameters can change throughout the night. Equation (7) therefore becomes

$$\frac{d[\text{HONO}]/[\text{NO}_2]}{dt} = \frac{S}{V} \frac{v}{4} \frac{g_{\text{NO}_2 \rightarrow \text{HONO}}(\text{RH})}{g_{\text{HONO}}(\text{RH})} \quad (8)$$

[43] The analytical solution for this equation, assuming that [HONO]/[NO<sub>2</sub>] = 0 at the beginning of the night ( $t = 0$ ), is

$$[\text{HONO}]/[\text{NO}_2] = \frac{S}{V} \frac{v}{4} \frac{g_{\text{NO}_2 \rightarrow \text{HONO}}(\text{RH})}{g_{\text{HONO}}(\text{RH})} \left( 1 - \exp\left(-\frac{S}{V} \frac{v}{4} \frac{g_{\text{NO}_2 \rightarrow \text{HONO}}(\text{RH})}{g_{\text{HONO}}(\text{RH})} t\right) \right) \quad (9)$$

[44] Equation (9) describes an exponential increase of the [HONO]/[NO<sub>2</sub>] ratio with a time constant of  $\frac{S}{V} \frac{v}{4} \frac{g_{\text{NO}_2 \rightarrow \text{HONO}}(\text{RH})}{g_{\text{HONO}}(\text{RH})}$ . It is interesting to note that this time constant depends only on the surface to volume ratio and the heterogeneous reaction probability of HONO but is independent of the NO<sub>2</sub> to HONO conversion probability.

[45] The dependence of the time constant on S/V requires a more detailed discussion. In a laboratory-type setting, S/V is clearly defined by the reaction vessel geometry. This approach is often also applied to the atmosphere by assuming a well-mixed nocturnal boundary layer with the ground as reactive surface. In this case, S/V is defined by the surface area of the ground and other reactive surfaces and the volume determined by the assumed height of the nocturnal boundary layer (NBL). However, the concept of a well-mixed boundary layer is often not justified during the night. Thus a volume cannot be easily defined [Stutz et al., 2002]. If the ground is the dominant reactive surface in the nocturnal boundary layer, the S/V cannot be interpreted directly as a surface to volume ratio since trace gases may be unevenly distributed with altitude. The degree of mixing throughout the boundary layer depends on the magnitude of vertical transport at



night. We therefore have to interpret  $S/V$  in equation (9) as a parameter that depends mainly on the strength of vertical mixing, i.e.,  $S/V$  is large during strong vertical stability (because the effective volume is small) and becomes smaller as the NBL becomes less stable. It should also be noted that if  $S/V$  is interpreted in this way, a change in vertical mixing during the night could lead to a change of  $S/V$ . It is also likely that aerosol particles contribute to the reactive surface in the NBL. In this case,  $S/V$  is a combination of the aerosol surface to volume ratio and the influence of vertical mixing.

[46] Equations (7) and (9) show that the  $\text{NO}_2$ -HONO system will ultimately reach a pseudo steady state (PSS), which is determined by the ratio of the two reaction probabilities  $g_{\text{NO}_2} \text{HONO}$  and  $g_{\text{HONO}}$

$$\frac{[\text{HONO}]}{[\text{NO}_2]}_{\text{PSS}} = \frac{1}{4} \frac{g_{\text{NO}_2} \text{HONO} \delta R : H : P}{g_{\text{HONO}} \delta R : H : P}; \quad \delta 10^6$$

[47] It is essential for our further interpretation to understand that the chemical system will always try to reach this PSS. The  $[\text{HONO}]/[\text{NO}_2]$  ratio can exceed the PSS value only if direct emissions add HONO to the system without adding a corresponding amount of  $\text{NO}_2$ . The system will then, however, move back into the PSS by an increased loss of HONO onto the surface.

[48] The fact that the HONO- $\text{NO}_2$  system moves into a PSS makes the interpretation of the influence of direct HONO emission difficult. As we have argued above, the true PSS lies between the emission corrected HONO mixing ratio,  $[\text{HONO}]$ , and the direct observation  $[\text{HONO}]_{\text{obs}}$  (equation (6)). As shown in the comparison of  $[\text{HONO}]_{\text{obs}}$  and  $[\text{HONO}]$  in Figures 2 and 3, the difference between these two values is typically between 0 and 10% and can reach 20% in extreme cases (not shown here). Keeping this systematic uncertainty in mind, we will use the emission-corrected HONO mixing ratio for the following interpretation of our data.

[49] From the discussion above, one expects that under meteorologically favorable conditions the  $[\text{HONO}]/[\text{NO}_2]$  ratio attains a constant level when the system reaches the PSS. This leveling off of the HONO-to- $\text{NO}_2$  ratio was indeed found during many nights in Nashville, Houston, and Phoenix, (section 3, Figures 1 and 2) and at other sites [e.g., Stutz et al., 2002]. Because of the strong influence of  $S/V$  and therefore vertical mixing, the time that is required to reach the PSS can, however, vary considerably. Our observations suggest that it is likely to find the  $\text{NO}_2$ -HONO system in a PSS at the end of a night. It is, however, also possible that the PSS is not reached, for example, if vertical mixing is too strong. Indeed, examples as in Figures 1 and 2 are not encountered in every night. In the further analysis we will therefore use the complete nocturnal data set, without considering the time of the night, to investigate the average behavior of the system.

#### 4.2. Order of HONO Loss

[50] We first test our hypothesis that the heterogeneous HONO loss is a first-order process. Figure 5 shows all nocturnal, emission-corrected HONO measurements during the three campaigns plotted against their respective  $\text{NO}_2$  mixing ratios. To determine the order of the HONO loss, we included three linear functions describing the

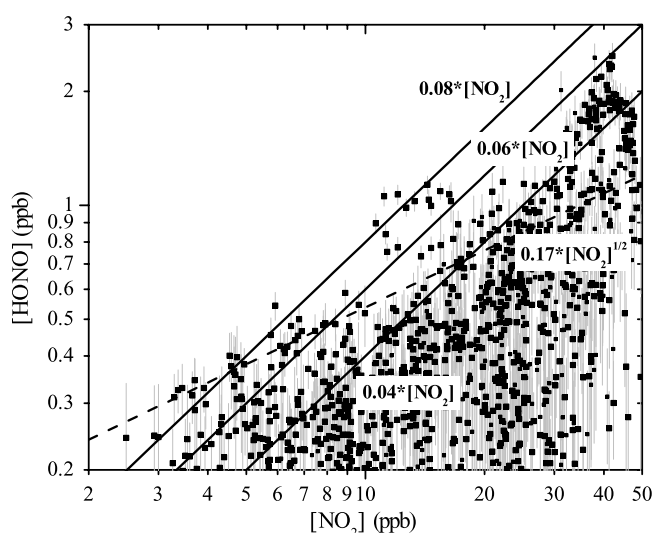


Figure 5. The maximum HONO mixing ratios from the three field experiments show a linear dependence of  $[\text{NO}_2]$ . The three continuous curves show a linear relation between  $[\text{HONO}]$  and  $[\text{NO}_2]$ , as predicted for the PSS in equation (10) with a heterogeneous reactivity ratio of 0.04, 0.06, and 0.08. For comparison, the expected curve for a second order loss of HONO is also included (dashed line).

dependence of  $[\text{HONO}]$  on  $[\text{NO}_2]$ , as predicted for the PSS by equation (10). The three functions were calculated for reaction probability ratios  $g_{\text{NO}_2} \text{HONO}/g_{\text{HONO}}$ , of 0.04, 0.06, and 0.08. The linear curves in Figure 5 describe the maximum values of  $[\text{HONO}]$  fairly well, considering that different reaction probability ratios may have been encountered. We also included the curve expected for a second order loss of HONO. In this case,  $[\text{HONO}]$  would depend on the square root of  $[\text{NO}_2]$  (compare with equation (7)). It is evident that this curve does not describe the maxima over the entire  $\text{NO}_2$  range in Figure 5. Only below 6 ppb  $\text{NO}_2$ , the quadratic dependence appears to describe the  $[\text{HONO}]$  maxima as well as the linear dependence. We conclude, based on our entire data set, that the assumption of a first order HONO loss is justified.

#### 4.3. RH Dependence of HONO Chemistry

[51] Figure 6 shows all nocturnal  $[\text{HONO}]/[\text{NO}_2]$  ratios observed during the three field experiments plotted against their respective relative humidities. It should be noted that we removed data of three nights from the Phoenix data set due to the influence of dust storms that showed extremely high  $[\text{HONO}]/[\text{NO}_2]$  ratios. The results of these nights are discussed by Wang et al. [2003a]. To supplement our data, we have also included the nocturnal  $[\text{HONO}]$  maxima observed by Harris et al. [1982] in the Los Angeles Basin. Our observations in Figure 6 are color-coded according to the time periods before and after midnight.

[52] To interpret Figure 6 we will rely on the theoretical discussion of the behavior of  $[\text{HONO}]$  and the  $[\text{HONO}]/[\text{NO}_2]$  ratio in section 4.1. For each RH,  $[\text{HONO}]/[\text{NO}_2]$  ratios can be influenced by the time of the night, the surface to volume ratio (equation (9)), and other parameters, such as advection. These dependencies lead to a range of  $[\text{HONO}]/[\text{NO}_2]$  values in Figure 6. Independent from



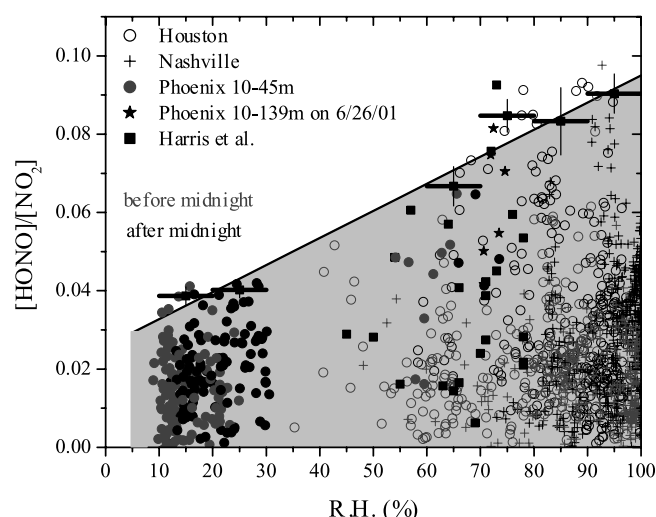


Figure 6.  $[\text{HONO}]/[\text{NO}_2]$  ratios versus RH for four different locations in the United States. Errors for  $[\text{HONO}]/[\text{NO}_2]$  are in the range 0.002–0.01 and were omitted in this plot for clarity. See color version of this figure at back of this issue.

these parameters is, however, that the  $\text{NO}_2$ -HONO system can reach a pseudo steady state, which is characterized by a maximum  $[\text{HONO}]/[\text{NO}_2]$  ratio. Concentrating solely on these maxima in Figure 6 will therefore eliminate much of the uncertainty connected with the influence of other parameters. To provide a better description of these maxima, we calculated the average of the five highest  $[\text{HONO}]/[\text{NO}_2]$  values in RH intervals of 10%. These averaged maxima are shown in Figure 6 as black horizontal bars, where the lengths of the bars indicate the RH interval. The standard deviation of the five maxima is also shown. Because data between 30 and 60% RH are sparse, the average of the maxima in these intervals is not displayed. Also shown in Figure 6 is a linear least squares fit through the averaged maxima.

[53] The maxima and their averages in Figure 6 show a clear dependence on the RH. While the maximum values in the 10–30% RH interval are in the range between 0.03 and 0.04, they reach 0.08–0.09 at RH between 70 and 95%. The few data points between 30 and 60% RH seem to have maximum ratios around 0.04–0.06. The averaged maxima lie on a line that describes the general behavior of all maxima well. It appears, however, that the  $[\text{HONO}]/[\text{NO}_2]$  ratios between 95 and 100% RH are lower than the values at 70–95% RH.

[54] The different symbols in Figure 6 show that the RH range between 10 and 35% is solely filled by data from Phoenix. Above 40% RH, all three campaigns and the data by [Harris et al., 1982] contribute. It is important to note that the humid night in Phoenix (Figure 3) agrees well with the values of Nashville and Houston around 70% RH. This night therefore provides the link between the four data sets and shows that the influence of the location on the  $[\text{HONO}]/[\text{NO}_2]$  ratio is less important than the dependence on RH.

[55] We can use equation (10) and the maximum  $[\text{HONO}]/[\text{NO}_2]$  ratios in Figure 6 to analyze the RH

dependence of the ratio between the heterogeneous reaction probabilities  $g_{\text{NO}_2! \text{ HONO}}(\text{RH})$  and  $g_{\text{HONO}}(\text{RH})$ . While we cannot determine which of the two parameters changes, we can conclude that the RH dependence of  $g_{\text{NO}_2! \text{ HONO}}(\text{RH})$  must be stronger than that of  $g_{\text{HONO}}(\text{RH})$  to explain the observations:

$$\frac{d g_{\text{NO}_2! \text{ HONO}}(\text{RH}) / d(\text{RH})}{g_{\text{NO}_2! \text{ HONO}}(\text{RH})} > \frac{d g_{\text{HONO}}(\text{RH}) / d(\text{RH})}{g_{\text{HONO}}(\text{RH})} \quad (11)$$

[56] It is important to note that there is currently little information of the RH dependence of  $g_{\text{HONO}}(\text{RH})$ . It is possible that this mechanism is only weakly dependent or even independent of RH, at least over a certain range of RH. In this case the observed change is purely due to the RH dependence of the  $\text{NO}_2$  to HONO conversion. Since the  $[\text{HONO}]/[\text{NO}_2]$  maxima in Figure 6 are linearly dependent on RH, we can conclude in this case that the  $\text{NO}_2$  to HONO conversion would be proportional to the RH,  $g_{\text{NO}_2! \text{ HONO}}(\text{RH}) / \text{RH}$ . This is in agreement with various laboratory results that find a linear dependence on RH. Syomin and Finlayson-Pitts [2003] recently reported that the HONO loss decreases with increasing RH between 0% and 50% RH, which would lead to a negative  $d(g_{\text{HONO}}(\text{RH}))/d(\text{RH})$ . If this is the case for the entire RH range, the RH dependence of  $g_{\text{NO}_2! \text{ HONO}}(\text{RH})$  could be less than linear, or  $g_{\text{NO}_2! \text{ HONO}}(\text{RH})$  could even be independent of RH.

[57] While the dry nights in Phoenix (e.g., Figure 4) seem to show that a PSS is reached, the low  $[\text{HONO}]$  levels make it difficult to prove that this is indeed the case. Since our interpretation thus far is based on the PSS assumption, we therefore need to consider the possibility that  $[\text{HONO}]/[\text{NO}_2]$  ratios are lower at lower RH because a PSS was not yet reached. A closer look at the exponential term in equation (9) reveals that a smaller  $g_{\text{HONO}}(\text{RH})$  at lower RH ( $d(g_{\text{HONO}}(\text{RH}))/d(\text{RH}) > 0$ ) would increase the time to reach the PSS. Because  $g_{\text{HONO}}(\text{RH})$  is also in the denominator in the first term of equation (9), a sole change in  $g_{\text{HONO}}(\text{RH})$  would, however, also lead to higher PSS  $[\text{HONO}]/[\text{NO}_2]$  ratios and thus to higher ratios during dry nights, which contradicts our observations. We can therefore conclude that  $g_{\text{NO}_2! \text{ HONO}}(\text{RH})$  also has to change with RH. The relation between the RH dependencies is somewhat more complicated, and we can distinguish between three different cases based on our observations that at  $\text{RH} > 70\%$  a PSS is reached. In the first,  $d(g_{\text{HONO}}(\text{RH}))/d(\text{RH})$  is smaller than  $d(g_{\text{NO}_2! \text{ HONO}}(\text{RH}))/d(\text{RH})$ , and the time to reach the PSS will be longer and the final  $[\text{HONO}]/[\text{NO}_2]$  ratio will be smaller at lower RH than at higher RH. This case would explain our observations and is in agreement with equation (11) and the explanation through a PSS. In the case that  $d(g_{\text{HONO}}(\text{RH}))/d(\text{RH})$  is approximately equal to  $d(g_{\text{NO}_2! \text{ HONO}}(\text{RH}))/d(\text{RH})$  the time to reach PSS is still longer at lower RH, but the PSS  $[\text{HONO}]/[\text{NO}_2]$  ratio will not change with RH. This case can, in principle, also explain our observations at low RH. The case of  $d(g_{\text{HONO}}(\text{RH}))/d(\text{RH})$  being larger than  $d(g_{\text{NO}_2! \text{ HONO}}(\text{RH}))/d(\text{RH})$  leads to an increase of the PSS at lower RH and, except for cases where the difference is small, will lead to higher  $[\text{HONO}]/[\text{NO}_2]$  ratios at the end of drier nights. From our consideration we can conclude that in the case a

PSS is not reached in the dry nocturnal boundary layer the following relation applies:

$$\frac{d(g_{\text{NO}_2/\text{HONO}} \delta R : \text{H} : \text{P})}{d\delta R : \text{H} : \text{P}} = \frac{d(g_{\text{HONO}} \delta R : \text{H} : \text{P})}{d\delta R : \text{H} : \text{P}}; \quad \delta 12\text{p}$$

[58] If the  $d(g_{\text{HONO}}(\text{RH}))/d(\text{RH})$  is negative, as suggested by Syomin and Finlayson-Pitts [2003], the steady state should be reached earlier at lower RH. In this case our observations in Phoenix would be in a PSS and equation (11) would apply.

[59] A dependence of S/V on RH could also influence the  $[\text{HONO}]/[\text{NO}_2]$  increase (equation (9)), depending on the involved reactive surface. In the case of aerosol surfaces, one expects larger S/V values at higher RH. In the case of the ground as reactive surface, S/V will depend on the magnitude of vertical mixing. Since the magnitude of vertical mixing in Phoenix was generally smaller (more stable boundary layers) than in Houston and Nashville, we expect higher S/V at lower RH. The contribution of the RH dependence is therefore not clear, but one can calculate that the available S/V from ground surfaces is higher in nocturnal urban environments than from the aerosol under normal conditions. Thus a slower increase of  $[\text{HONO}]/[\text{NO}_2]$  due to a change in S/V is not expected for drier conditions.

[60] In summary, we can conclude that the RH dependence of the  $[\text{HONO}]/[\text{NO}_2]$  maxima observed in urban areas is due to the dependence of the reaction and uptake probabilities of  $\text{NO}_2$  and HONO. While we can only determine the ratio of the two probabilities, our derivation indicates that the dependence of the reaction probability of  $\text{NO}_2$  on RH is larger than that of the uptake probability of HONO.

#### 4.4. Comparison to Literature

[61] Earlier work on HONO formation often showed a first-order dependence of the formation rate on the concentration of water vapor [Jenkin et al., 1988; Pitts et al., 1984b; Sakamaki et al., 1983; Svensson et al., 1987]. Most of these studies were performed in laboratory settings under conditions of constant temperatures. The water vapor concentration and thus the formation of HONO was therefore proportional to the RH.

[62] Other studies have suggested that the parameter that influences the  $\text{NO}_2$  to HONO conversion is the amount of surface adsorbed water [Finlayson-Pitts et al., 2003; Kleffmann et al., 1998]. In a first approximation, one would expect that the amount of surface adsorbed water is proportional to the RH. Saliba et al. [2001], for example, determined that the number of water monolayers on glass followed a Brunauer, Emmett, and Teller (BET) isotherm. The data shows that the dependence can be approximated by a linear function between 10 and 70% and increases more strongly at higher RH. Lammel [1999] shows that the water coverage of various materials, expressed as number of monolayers of water, increases steadily with RH. In the case of stone and soil, the coverage around 20% RH is around 1 monolayer. The coverage increases to 3.5 monolayers at 80% RH. Above 80% RH, the coverage rapidly increases. Goodman et al. [2001] found a similar behavior on oxide particles. Qualitatively, the results of the different studies agree and the water coverage can therefore clearly be related to the RH. We

want to caution, however, about taking too literal a view of a monolayer for atmospheric surfaces. The complex surface structure of natural surfaces will most likely lead to a mixture of areas with little surface adsorbed water and areas with many layers of water molecules. The functional dependence of the water coverage on the RH resulting from this averaging is not clear. For our case we will therefore assume that the water coverage is proportional to the RH below 80% RH. Above 95% RH a change in coverage may occur [Lammel, 1999], which could explain the lower  $[\text{HONO}]/[\text{NO}_2]$  ratios observed in this range. Below 10% RH, where less than one monolayer is present on the surface [Lammel, 1999; Goodman et al., 2001], the amount of adsorbed water decreases rapidly to zero at 0% RH. One would thus expect a fast decrease of the  $[\text{HONO}]/[\text{NO}_2]$  ratios in Figure 6 below 10% RH. Because nocturnal RH is typically above 10% in the atmosphere, no information for HONO and  $\text{NO}_2$  in this range is available.

[63] As we discussed above, under the assumption that the HONO uptake is independent or only weakly dependent on RH, our data shows a proportionality of the  $\text{NO}_2$  to HONO conversion probability and the RH,  $g_{\text{NO}_2/\text{HONO}}/\text{RH}$ . It therefore appears that our results are in agreement with the laboratory findings that predict a first-order dependence on the RH or the amount of surface-adsorbed water. In contrast, the recent observation of a negative RH dependence of  $g_{\text{HONO}}(\text{RH})$  by Syomin and Finlayson-Pitts, [2003] imply that the  $g_{\text{NO}_2/\text{HONO}}$  dependence on RH could be less than linear.

[64] Saliba et al. [2001] describe that in the uptake of NO onto a surface previously exposed to  $\text{HNO}_3$ , the maximum uptake occurs around a 3 monolayer coverage. They explain their results by a particular hydrogen bonding of  $\text{HNO}_3$  in the surface layer. While the results of Saliba et al. [2001] apply to a different chemical reaction, surface adsorbed  $\text{HNO}_3$  is also expected to play a role in the HONO loss on surfaces (see reaction (R5)). Our data, however, shows no clear change around a 3 monolayer coverage expected at 50% RH. Considering that natural surfaces will not have a uniform water coverage, as the glass surfaces in the study by Saliba et al. [2001], we suspect that any possible effect was averaged out to an extent that it would not be visible in our observations.

#### 5. Conclusions

[65] Measurements of  $[\text{NO}_2]$ ,  $[\text{HONO}]$ , and RH from three different locations were analyzed with respect to the dependence of HONO chemistry on RH. Examples of the nocturnal behavior of  $[\text{HONO}]$  and the  $[\text{HONO}]/[\text{NO}_2]$  ratio show a leveling off in the later part of the night. Following earlier results by Stutz et al. [2002], we interpret this behavior as a pseudo steady state (PSS) between the heterogeneous conversion of  $\text{NO}_2$  to HONO and the loss of HONO on surfaces. A simplified mathematical description shows that the PSS  $[\text{HONO}]/[\text{NO}_2]$  ratio solely depends on the ratio of the heterogeneous reaction probabilities of  $\text{NO}_2$  and HONO,  $g_{\text{NO}_2/\text{HONO}}/g_{\text{HONO}}$ . The surface to volume ratio, which can be interpreted as a measure for vertical mixing if the ground is the reactive surface, and the reactive HONO uptake,  $g_{\text{HONO}}$ , influence the time constant that is needed to reach the PSS.

[66] Based on these theoretical considerations, we associate the observed maximum  $[\text{HONO}]/[\text{NO}_2]$  ratios at various RH with the PSS of the  $\text{NO}_2$ -HONO system. A plot of all the  $[\text{HONO}]/[\text{NO}_2]$  ratios determined at night in the three field experiments clearly shows that the maximum  $[\text{HONO}]/[\text{NO}_2]$  ratio depends on the RH. From this observation we can conclude that the dependence on RH of the reaction probability of the  $\text{NO}_2$  to HONO conversion is stronger than that of the loss of HONO. In the case that the reactive HONO uptake probability,  $g_{\text{HONO}}$ , is independent of RH, our data would predict a linear dependence of  $g_{\text{NO}_2/\text{HONO}}$  on RH, in agreement with laboratory observations. For a negative RH dependence of  $g_{\text{HONO}}$ , [Syomin and Finlayson-Pitts, 2003] our results imply that  $g_{\text{NO}_2/\text{HONO}}$  is less dependent on RH or perhaps even independent of RH.

[67] Many air pollution models currently employ a simplified  $\text{NO}_2$  to HONO conversion mechanism that does not take RH dependence into account. Aumont et al. [2003], for example, parameterize HONO formation solely as a first-order conversion of  $\text{NO}_2$ . A parameterization omitting the influence of the RH, or surface-adsorbed water, will lead to a number of misrepresentations of HONO formation. It will, for example, overestimate the daytime HONO formation, since the RH is typically lower during day than during night. It also has implications for the applicability of a model to different locations such as those shown in our study.

[68] The apparent dependence of the  $\text{NO}_2$  to HONO conversion on RH in environments with natural surfaces needs further investigation. Our study shows that water, most likely in its surface adsorbed form, can have a considerable influence on heterogeneous reactions in the atmosphere. It is very likely that a RH dependence of other heterogeneous reactions can also be found on natural surfaces.

[69] Acknowledgments. This study was supported by the NOAA Health of the Atmosphere Research Program, the EPA-Southern Oxidant Study program (grant 1995-1786-09), the Texas Natural Resource Conservation Commission, (grant 582-2-48650), and the Department of Energy (grant DE-FG03-01ER63094).

## References

- Ackermann, R. (2000), Auswirkungen von Kraftfahrzeugemissionen in der urbanen Atmosphäre, Ph.D. thesis, Univ. of Heidelberg, Heidelberg, Germany.
- Alicke, B., U. Platt, and J. Stutz (2002), Impact of nitrous acid photolysis on the total hydroxyl radical budget during the Limitation of Oxidant Production/Pianura Padana Produzione di Ozono study in Milan, *J. Geophys. Res.*, 107(D22), 8196, doi:10.1029/2000JD000075.
- Alicke, B., A. Geyer, A. Hofzumahaus, F. Holland, S. Konrad, H.-W. Pöhl, J. Scher, J. Stutz, A. Volz-Thomas, and U. Platt (2003), OH formation by HONO photolysis during the BERLIOZ experiment, *J. Geophys. Res.*, 108(D4), 8247, doi:10.1029/2001JD000579.
- Ammann, M., M. Kalberer, D. T. Jost, L. Tobler, E. Rossler, D. Piguet, H. W. Gaggeler, and U. Baltensperger (1998), Heterogeneous production of nitrous acid on soot in polluted air masses, *Nature*, 395, 157–160.
- Andres-Hernandez, M. D., J. Notholt, J. Hjorth, and O. Schrems (1996), A DOAS study on the origin of nitrous acid at urban and non-urban sites, *Atmos. Environ.*, 30(2), 175–180.
- Aumont, B., F. Chervier, and S. Laval (2003), Contribution of HONO sources to the  $\text{NO}_2/\text{HO}_x/\text{O}_3$  chemistry in the polluted boundary layer, *Atmos. Environ.*, 37(4), 487–498.
- Barney, W. S., and B. J. Finlayson-Pitts (2000), Enhancement of  $\text{N}_2\text{O}_4$  on porous glass at room temperature: A key intermediate in the heterogeneous hydrolysis of  $\text{NO}_2$ , *J. Phys. Chem. A*, 104(2), 171–175.
- Bongartz, A., J. Kames, U. Schurath, C. George, P. Mirabel, and J. L. Ponche (1994), Experimental determination of HONO mass accommodation coefficients using 2 different techniques, *J. Atmos. Chem.*, 18(2), 149–169.
- Calvert, J. G., G. Yarwood, and A. M. Dunker (1994), An evaluation of the mechanism of nitrous acid formation in the urban atmosphere, *Res. Chem. Interim.*, 20(3), 463–502.
- Finlayson-Pitts, B. J., and J. N. Pitts (2000), *Chemistry of the Upper and Lower Atmosphere: Theory, Experiments and Applications*, Academic, San Diego, Calif.
- Finlayson-Pitts, B. J., L. M. Wingen, A. L. Sumner, D. Syomin, and K. A. Ramazan (2003), The heterogeneous hydrolysis of  $\text{NO}_2$  in laboratory systems and in outdoor and indoor atmospheres: An integrated mechanism, *Phys. Chem. Chem. Phys.*, 5, 223–242.
- Gerecke, A., A. Thielmann, L. Gutzwiller, and M. J. Rossi (1998), The chemical kinetics of HONO formation resulting from heterogeneous interaction of  $\text{NO}_2$  with flame soot, *Geophys. Res. Lett.*, 25(13), 2453–2456.
- Goodman, A. L., G. M. Underwood, and V. H. Grassian (1999), Heterogeneous reaction of  $\text{NO}_2$ : Characterization of gas-phase and adsorbed products from the reaction,  $2\text{NO}_2(\text{g}) + \text{H}_2\text{O}(\text{a}) \rightarrow \text{HONO}(\text{g}) + \text{HNO}_3(\text{a})$  on hydrated silica particles, *J. Phys. Chem. A*, 103(36), 7217–7223.
- Goodman, A. L., E. T. Bernard, and V. H. Grassian (2001), Spectroscopic study of nitric acid and water adsorption on oxide particles: Enhanced nitric acid uptake kinetics in the presence of adsorbed water, *J. Phys. Chem. A*, 105(26), 6443–6457.
- Harris, G. W., W. P. L. Carter, A. M. Winer, J. N. Pitts, U. Platt, and D. Perner (1982), Observations of nitrous acid in the Los Angeles atmosphere and implications for the predictions of ozone-precursor relationships, *Environ. Sci. Technol.*, 16(2), 414–419.
- Harrison, R. M., J. D. Peak, and G. M. Collins (1996), Tropospheric cycle of nitrous acid, *J. Geophys. Res.*, 101(D9), 14,429–14,439.
- Jenkin, M. I., R. A. Cox, and D. J. Williams (1988), Laboratory studies of the kinetics of formation of nitrous acid from the thermal reaction of nitrogen dioxide and water vapour, *Atmos. Environ.*, 22(3), 487–498.
- Kaiser, E. W., and C. H. Wu (1977), A kinetic study of the gas phase formation and decomposition reactions of nitrous acid, *J. Phys. Chem.*, 81(18), 1701–1706.
- Kalberer, M., M. Ammann, F. Arens, H. W. Gaggeler, and U. Baltensperger (1999), Heterogeneous formation of nitrous acid (HONO) on soot aerosol particles, *J. Geophys. Res.*, 104(D11), 13,825–13,832.
- Kessler, C. (1984), Gasförmige salpetrige Säure ( $\text{HNO}_2$ ) in der belasteten Atmosphäre, Ph.D. thesis, University of Cologne, Köln, Germany.
- Kirchstetter, T. W., R. A. Harley, and D. Littlejohn (1996), Measurement of nitrous acid in motor vehicle exhaust, *Environ. Sci. Technol.*, 30(9), 2843–2849.
- Kitto, A. M. N., and R. M. Harrison (1992), Nitrous and nitric acid measurements at sites in South-East England, *Atmos. Environ.*, 26(2), 235–241.
- Kleffmann, J., K. H. Becker, and P. Wiesen (1998), Heterogeneous  $\text{NO}_2$  conversion processes on acid surfaces: Possible atmospheric implications, *Atmos. Environ.*, 32(16), 2721–2729.
- Kleffmann, J., K. H. Becker, M. Lackhoff, and P. Wiesen (1999), Heterogeneous conversion of  $\text{NO}_2$  on carbonaceous surfaces, *Phys. Chem. Chem. Phys.*, 1(24), 5443–5450.
- Kurtenbach, R., K. H. Becker, J. A. G. Gomes, J. Kleffmann, J. C. Lorzer, M. Spittler, P. Wiesen, R. Ackermann, A. Geyer, and U. Platt (2001), Investigations of emissions and heterogeneous formation of HONO in a road traffic tunnel, *Atmos. Environ.*, 35(20), 3385–3394.
- Lammel, G. (1999), Formation of nitrous acid: Parameterisation and comparison with observations, Rep. 286, 36 pp., Max-Planck-Inst. für Meteorol., Hamburg, Germany.
- Longfellow, C. A., A. R. Ravishankara, and D. R. Hanson (2000), Reactive and nonreactive uptake on hydrocarbon soot:  $\text{HNO}_3$ ,  $\text{O}_3$ , and  $\text{N}_2\text{O}_5$ , *J. Geophys. Res.*, 105(D19), 24,345–24,350.
- Mertes, S., and A. Wahner (1995), Uptake of nitrogen dioxide and nitrous acid on aqueous surfaces, *J. Phys. Chem.*, 99(38), 14,000–14,006.
- Pitts, J. N., H. W. Biermann, A. M. Winer, and E. C. Tuazon (1984a), Spectroscopic identification and measurement of gaseous nitrous acid in dilute auto exhaust, *Atmos. Environ.*, 18(4), 847–854.
- Pitts, J. N., E. Sanhueza, R. Atkinson, W. P. L. Carter, A. M. Winer, G. W. Harris, and C. N. Plum (1984b), An investigation of the dark formation of nitrous acid in environmental chambers, *Int. J. Chem. Kinet.*, XVI, 919–939.
- Platt, U. (1986), The origin of nitrous and nitric acid in the atmosphere, in *Chemistry of Multiphase Atmospheric Systems*, edited by W. Jaeschke, pp. 299–319, Springer-Verlag, New York.
- Platt, U. (1994), Differential Optical Absorption Spectroscopy (DOAS), in *Monitoring by Spectroscopic Techniques*, edited by M. W. Sigrist, John Wiley, Hoboken, N.J.



- Sakamaki, F., S. Hatakeyama, and H. Akimoto (1983), Formation of nitrous acid and nitric oxide in the heterogeneous dark reaction of nitrogen dioxide and water vapor in a smog chamber, *Int. J. Chem. Kinet.*, 1013–1029.
- Saliba, N. A., M. Mochida, and B. J. Finlayson-Pitts (2000), Laboratory studies of sources of HONO in polluted urban atmospheres, *Geophys. Res. Lett.*, 27(19), 3229–3232.
- Saliba, N. A., H. Yang, and B. J. Finlayson-Pitts (2001), Reaction of gaseous nitric oxide with nitric acid on silica surfaces in the presence of water at room temperature, *J. Phys. Chem. A*, 105(45), 10,339–10,346.
- Sjoman, A., and M. Ferm (1985), Measurement of nitrous acid in an urban area, *Atmos. Environ.*, 19(6), 985–992.
- Spindler, G., E. Brüggemann, and H. Herrmann (1999), Nitrous acid concentration measurements and estimation of dry deposition over grassland in Eastern Germany, in *Proceedings of EUROTRAC Symposium 98*, vol. 2, edited by P. M. Borrell and P. Borrell, pp. 218–222, Wentworth Inst. of Technol., Boston, Mass.
- Stutz, J., B. Alicke, and A. Neftel (2002), Nitrous acid formation in the urban atmosphere: Gradient measurements of NO<sub>2</sub> and HONO over grass in Milan, Italy, *J. Geophys. Res.*, 107(D18), 8192, doi:10.1029/2001JD000390.
- Svensson, R., E. Ljungström, and O. Lindqvist (1987), Kinetics of the reaction between nitrogen dioxide and water vapour, *Atmos. Environ.*, 21(7), 1529–1539.
- Syomin, D. A., and B. J. Finlayson-Pitts (2003), HONO decomposition on borosilicate glass surfaces: Implications for environmental chamber studies and field experiments, *Phys. Chem. Chem. Phys.*, 5(23), 5236–5242.
- Syomin, D., K. A. Ramazan, and B. J. Finlayson-Pitts (2002), HONO reactions on clean and nitric acid doped glass surfaces, *Eos Trans. AGU*, 83(47), Fall Meet. Suppl., Abstract A22B-0081.
- TenBrink, H. M., and H. Spoelstra (1998), The dark decay of HONO in environmental (SMOG) chambers, *Atmos. Environ.*, 32(2), 247–251.
- Wang, S., R. Ackermann, J. D. Fast, C. W. Spicer, M. Schmeling, and J. Stutz (2003a), Atmospheric observations of enhanced NO<sub>2</sub>-HONO conversion on mineral dust particles, *Geophys. Res. Lett.*, 30(11), 1595, doi:10.1029/2003GL017014.
- Wang, S., R. Ackermann, A. Geyer, J. C. Doran, W. J. Shaw, J. D. Fast, C. W. Spicer, and J. Stutz (2003b), Vertical variation of nocturnal NO<sub>x</sub> chemistry in the urban environment of Phoenix, paper presented at Annual Meeting, Am. Meteorol. Soc., Long Beach, Calif.
- Williams, E. J., et al. (1998), Intercomparison of ground-based NO<sub>y</sub> measurement techniques, *J. Geophys. Res.*, 103(D17), 22,261–22,280.
- R. Ackermann, B. Alicke, A. Geyer, J. Stutz, and S. Wang, Department of Atmospheric Sciences, University of California, Los Angeles, CA 90095-1565, USA. (ralf.ackermann@al-lightning.com; bjoern.alicke@web.de; andreas@atmos.ucla.edu; jochen@atmos.ucla.edu; shw@atmos.ucla.edu)
- J. D. Fast, Pacific Northwest National Laboratory, Richland, WA 99352, USA. (jerome.fast.pnl.gov)
- C. W. Spicer, Battelle Science and Technology International, Columbus, OH 43201-2693, USA. (spicerc@battelle.org)
- E. J. Williams, Aeronomy Laboratory, National Oceanic and Atmospheric Administration, Boulder, CO 80309, USA. (eric@al.noaa.gov)
- A. B. White, Environmental Technology Laboratory, National Oceanic and Atmospheric Administration, Boulder, CO 80309, USA. (allen.b.white@noaa.gov)



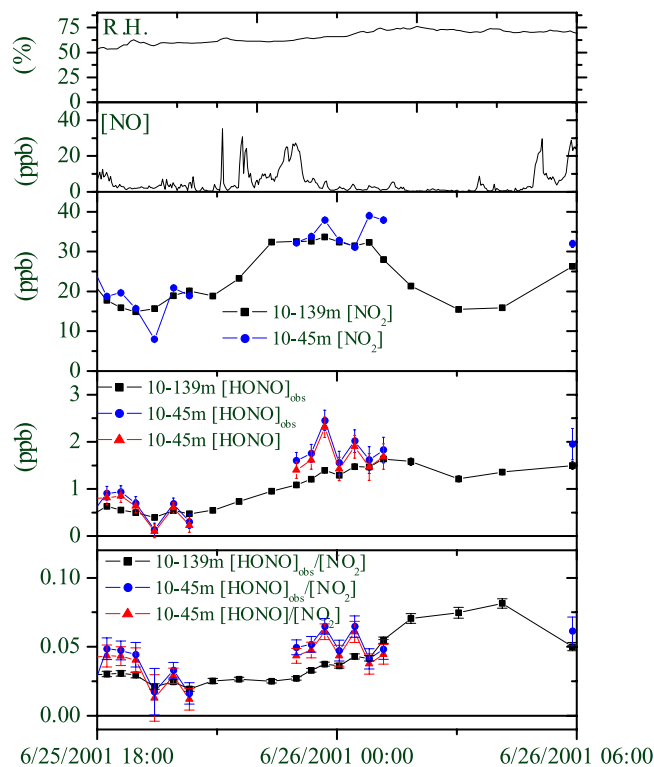


Figure 3. Behavior of [NO], [NO<sub>2</sub>], [HONO], and RH during one night in Phoenix, Arizona. The night is characterized by relatively high nocturnal RH.

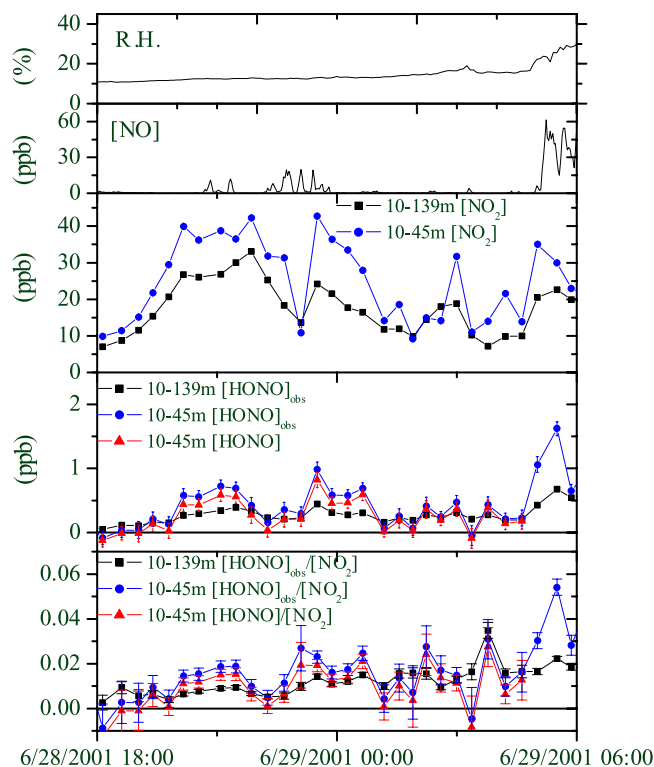


Figure 4. Behavior of [NO], [NO<sub>2</sub>], [HONO], and RH during one night in Phoenix, Arizona. The night is characterized by very low nocturnal RH below 35%. [HONO] is not shown after 0430, when the onset of photolysis and strong emissions during rush hour make an emission correction unreliable.

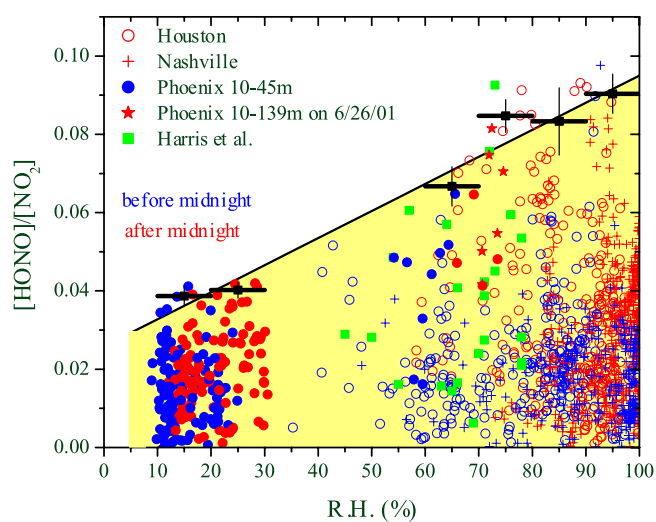


Figure 6.  $[\text{HONO}]/[\text{NO}_2]$  ratios versus RH for four different locations in the United States. Errors for  $[\text{HONO}]/[\text{NO}_2]$  are in the range 0.002–0.01 and were omitted in this plot for clarity.